



# Combined thrust radial bearing of a submarine main shaft – Design and analysis of failure



Michał Wasilczuk<sup>a,\*</sup>, Filip Wasilczuk<sup>b</sup>

<sup>a</sup> Gdańsk University of Technology, Faculty of Mechanical Engineering, Narutowicza 11/12, 80-229 Gdańsk, Poland

<sup>b</sup> Institute of Fluid Flow Machinery, Polish Academy of Sciences, Address: Fiszerka 14, 80-231 Gdańsk, Poland

## ARTICLE INFO

### Keywords:

Submarine  
Tilting pad thrust bearing  
Bearing failure  
Autonomous lubricating system

## ABSTRACT

This paper presents an analysis of the combined thrust radial bearing of a submarine propulsion shaft. The lubrication system of the bearing is based on a fixed ring. The efficiency of the lubrication system depends on the shaft speed and temperature, which affects oil viscosity. In turn, the thrust bearing load also depends on the rotational speed of the shaft, because as the speed increases, the drag of the ship increases simultaneously, but this increase in load is accompanied by the increase of load capacity of the hydrodynamic thrust bearing. The analysis made it possible to assess the causes of bearing failure and formulate recommendations for bearing operation.

## 1. Marine thrust bearings and their development

The thrust bearing is a critical component of a ship propulsion system because it transfers the thrust force from the ship's propeller to its hull. Soon after the invention of hydrodynamic tilting pad thrust bearings, around the beginning of 20th century, they were independently introduced to marine propulsion systems by Michell and Kingsbury, bringing unprecedented reliability and radically decreasing losses. The history and development of naval thrust bearings was thoroughly described by Simmons and Henderson [1]. Thrust bearings installed in submersible vessels are similar to general purpose marine thrust bearings, however the design criteria is more sophisticated. The need for a light and compact design becomes more profound in the case of severe operating conditions, such as the need to function with a flooded bearing compartment for certain amounts of time, sudden maneuvers or withstanding atypical ship orientation, e.g. inclination. Due to these reasons, the bearings of submersible vessels are an area of current research. Bearing manufacturers conduct theoretical and experimental research and execute development programs – such as testing the bearing ability to operate in an atypical position in a specially built rig (Fig. 1) [2].

The reduction of submarine vibration and noise is another crucial design goal, so a lot of effort is put into researching this subject. A review of various methods of reducing acoustic signature is presented in [3], and a review of the methods used to reduce vibration in the propulsion system in [4]. Thrust bearing is important in this aspect, because research has shown that the thrust bearing base serves as the main path to transfer longitudinal vibration from the propeller when its blades rotate through a non-uniform wake [5]. Special sliding layers made from rubber have been tested in [6], PTFE lined thrust bearings reported in [7] may also ensure the quiet running of the bearing. In addition, hydraulic resonance systems are studied and introduced to dampen vibrations and change their frequency in [3,4,5]. Recently, active methods of reducing acoustic signature are also being incorporated, as shown in [3].

The work presented here was aimed at finding the reasons for instances of particular thrust bearing failures, therefore the topics

\* Corresponding author.

E-mail addresses: [michal.wasilczuk@pg.edu.pl](mailto:michal.wasilczuk@pg.edu.pl) (M. Wasilczuk), [fwasilczuk@imp.gda.pl](mailto:fwasilczuk@imp.gda.pl) (F. Wasilczuk).

<https://doi.org/10.1016/j.engfailanal.2020.104651>

Received 26 February 2020; Received in revised form 1 June 2020; Accepted 2 June 2020

Available online 10 June 2020

1350-6307/ © 2020 The Authors. Published by Elsevier Ltd. This is an open access article under the CC BY license (<http://creativecommons.org/licenses/by/4.0/>).

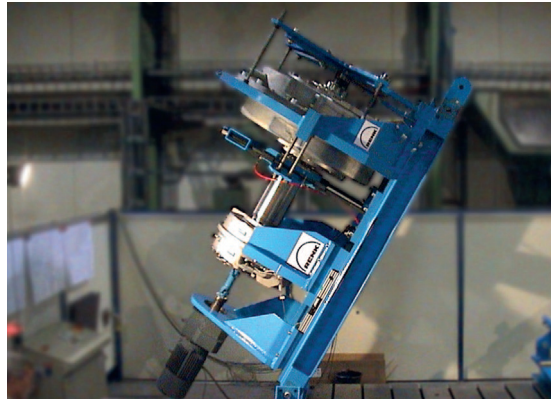


Fig. 1. Facility for testing operation of submarine thrust bearings in various positions [2].

mentioned above were not studied in detail, and were carried out in accordance with the general rules of Root Cause Analysis (RCA) as described in a paper dealing with the failure of a keyway in a gear-reduction shaft [8]. The steps comprise of: description of failure, recording of failure history, failure hypotheses; analysis, investigation results and as a result causes of failure and preventive measures.

Understanding of marine failures and military equipment is of vital importance, because of clear requirements concerning serviceability and difficulties in repairing when in off-shore conditions.

Failures of tilting pad thrust bearings are not common, however some cases have been described in literature, for example the paper by Iliev [9] can be mentioned, where the author, after a systematic analysis of a case of hydro-generator thrust bearing failure, found that the most probable reason was the misalignment of pads, leading to the overload of some of the pads and rupture of the oil film. Another case described in literature is the problem of sediment which erodes the surfaces of turbines, including the labyrinth seals. Increased clearances caused overload of the thrust bearing and accelerated wear of many turbine components [10].

## 2. System description

The submarine's thrust block is of a conventional design. The tilting pad thrust bearing is combined with two radial bearings in one housing. For operational reasons it also common to design a compact bearing block, which is autonomous, as far as lubrication is concerned. Therefore a common housing of all four bearings comprises of an autonomous lubricating system. The cross section of the combined bearing is shown in Fig. 2 [11]. Pads of both thrust bearings and journal bearings are lined with a conventional and widely used tin-based bearing alloy (Babbitt), of which the main attributes are [12]:

- (a) conformability allowing to take up misalignments due to relatively low hardness;
- (b) it is fairly inert – not easily corroded by hot oil;
- (c) embeddability allowing hard dirt particles to be buried into the bearing material – thus avoiding scoring of the journal
- (d) low melting point – in the event of incipient seizure it can melt locally and prevents serious damage.

The shaft with an integral collar is axially positioned with two tilting pad thrust bearings. The bearing pad is marked with No 3. The radial position of the shaft is provided by two cylindrical radial bearings. The lower part of the housing is filled with oil so that the lower section of the collar is immersed in oil. A cooler (37) accommodates the excessive heat generated in the bearings. The housing is sealed on both sides with the use of seal rings.

The operation of the lubrication system is as follows - the lower part of the thrust collar is immersed in oil. The movement of the collar causes the oil to move on its outer surface. An oil scraper (6) is installed in the upper part of the housing. The oil scraped from the disc flows into the pockets attached to the bearing housing (10). Oil flows out of the pockets by gravity, through a 20 mm inclined hole which is visible in the cross section in Fig. 2. The oil then lubricates the radial bearings and at the same time, through two axial grooves with a cross section of approximately 8 mm × 6 mm made in the bearing housing horizontal split plane (not shown in Fig. 2), flows along the shaft to the thrust collar and is further distributed among the pads due to centrifugal and viscous forces.

A characteristic feature of the propeller shaft thrust bearings is the dependence of load on speed - the propulsion force generated by the screw is proportional to the square of the rotational speed of the screw, according to the following formula [13]:

$$T = K_T \times \rho \times D^4 \times n^2 \quad (1)$$

where

- T – propeller thrust [N]
- $K_T$  – thrust coefficient
- $\rho$  – water density [kg/m<sup>3</sup>]
- D – propeller diameter [m]

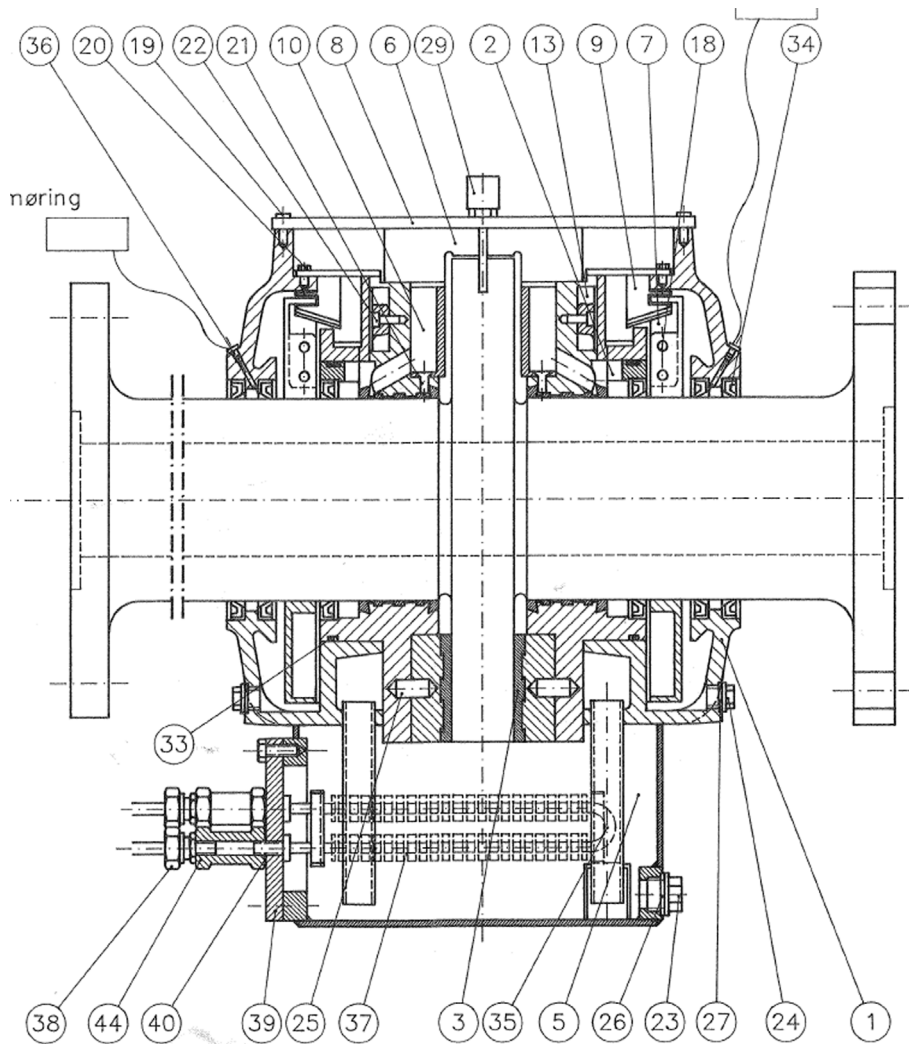


Fig. 2. Cross section through a combined thrust radial bearing [11].

$n$  – rotational speed [1/s]

In addition, it is characteristic for hydrodynamic bearings that the load carrying capacity increases with the increase of the sliding speed. Thus, with the increase of vessel velocity. An increasing load can be carried by the thrust bearing.

However, in a submarine thrust bearing, a hydrostatic component dependent on the depth of immersion is also present. Thus, in a submersible vessel the most unfavourable operating condition is slow motion in maximum immersion, because then with the hydrostatic component of substantial value and at a low shaft speed the bearing hydrodynamic capacity may be insufficient. That is why a hydrostatic auxiliary system is sometimes used in submarine thrust bearing [1]. Also, in some cases operating instructions put restrictions on the bearing rotational speed as a function of the depth of immersion, Fig. 3 [14].

### 3. Failure description

A failure of the thrust bearing of a submarine occurred during commissioning trials after the submarine's general overhaul. The circumstances of the failure are only vaguely known – it occurred when the rotational speed of the shaft was increased from 210 rpm to the maximum speed of 270 rpm, and the oil temperature was approximately 30 °C.

The photographs of the damaged bearing pads are shown in Fig. 4 and Fig. 5, it can be seen that the pads are damaged to a varying extent, with melted bearing alloy on all of them, but mostly visible on pads No 2, 4, 5, 6, 7 and 8, and black marks of burnt oil appearing on only some of the pads, namely on pads no 1, 3, 4 and 9. It seems that on the pads showing black marks from the burnt oil, the extent of melting is somewhat lesser. Pad no 4 seems to be the only one where quite heavy melting is combined with black marks. In Fig. 5, one can observe the characteristic image of deposits of melted alloy at the inlet zone of the downstream pad, which had been transferred from the upstream pad - in this case from Pad No 1 to Pad No 2. It is worth mentioning that the extent of

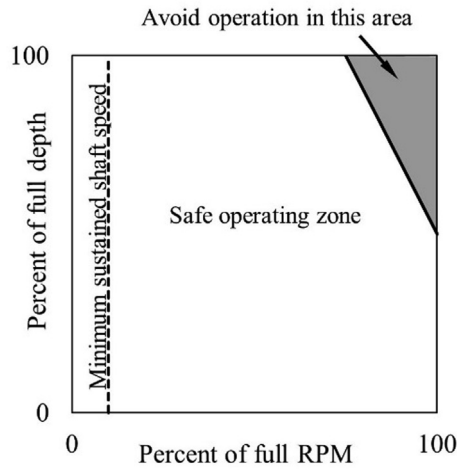


Fig. 3. Example of operating limits of a submarine thrust bearing [14].

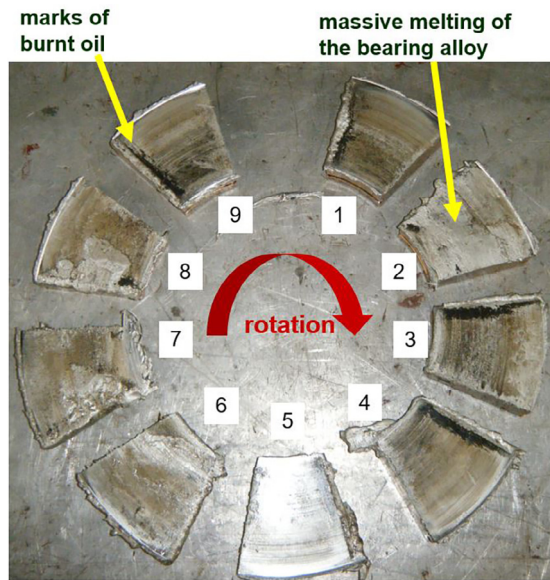


Fig. 4. Top view of bearing pads after the failure.

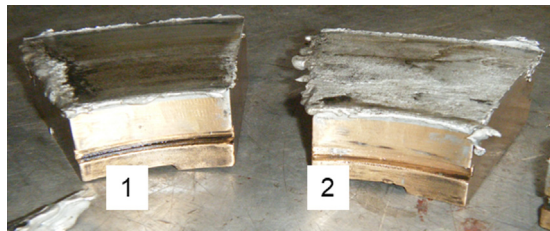


Fig. 5. Side view of two bearing pads after the failure.

destruction may also be affected by uneven load distribution between the pads.

#### 4. Bearing design analysis

The analyzed hydrodynamic tilting pad bearing is quite standard in design, comprising of 9 pads with off-set line support. Pads are made from bronze and are lined with a thick, 9 mm layer of Babbitt. The lubricant is Shell Gadinia 40 oil used for medium speed

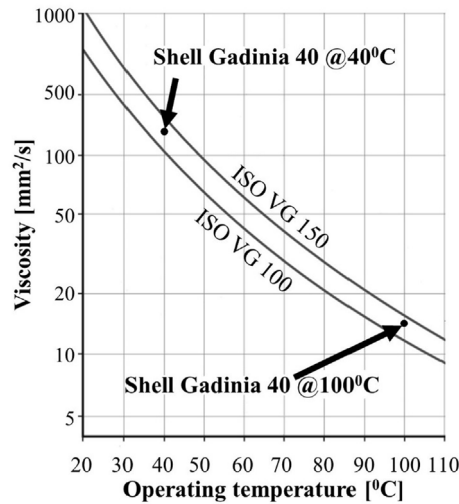


Fig. 6. Viscosity vs. temperature chart of lubricating oils [16].

marine diesel engines [15], for which kinematic viscosity is 139.0 mm<sup>2</sup>/s and 14.4 mm<sup>2</sup>/s for 40 °C and 100 °C, respectively. Comparing these values to ISO VG (Viscosity Grade) charts (Fig. 6) the lubricant viscosity can be considered equivalent to ISO VG-150.

Based on the bearing load at the surface and at 270 rpm, and a hydrostatic component which amounts to 85 kN at the submarine's maximum immersion depth of 180 m (given in the submarine specifications [10]), a simplified relationship between propulsion force and shaft rotational speed for the analysed submarine can be reproduced, as presented in Fig. 7. The most important technical data of the bearing is collected in Table 1.

5. Bearing operating parameters

Existing international standard [17] allows for the assessment of bearing design, based on the solution of Reynolds equation. The standard solution utilizes some additional assumptions, such as isoviscous lubricant flow, lack of pad deformations, oil gap completely filled with the lubricant. Such assumptions are widely used in isothermal theory of hydrodynamic lubrication. The standard also gives recommendations of threshold values of crucial parameters – film thickness and maximum temperature, taken from values well-established by engineering practice. In this case there is no data concerning temperature measurements, but the limit of the film thickness, based on the transition value to the mixed friction regime with a safety factor of 1.25, can be calculated:

$$h_{lim} = 1.25 \sqrt{\frac{D \times R_z}{12000}} = 10.7 \times 10^{-6} m \tag{2}$$

where  $D$  is the mean diameter of the bearing equal to 0.352 m.

$R_z$  is the roughness parameter equal to  $0.64 \times 10^{-6}$  m, according to the bearing drawings.

On the other hand, according to [17], the expected minimum film thickness and bearing maximum temperature can be evaluated, with the use of the following formula:

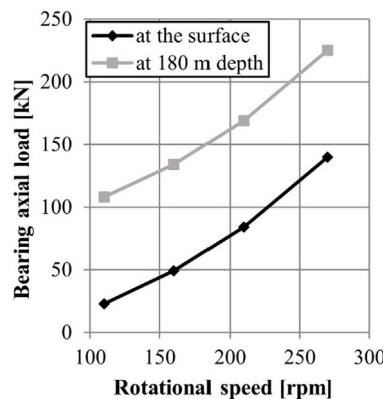


Fig. 7. Thrust bearing load [kN] on the surface and in maximum submersion depth as a function of shaft rotational speed [rpm].



**Table 1**  
Main specifications of the submarine thrust bearing.

Parameter	Value
Outer diameter/ inner diameter	447 mm/257 mm
Number of pads	9
Rotational speed	Up to 270 rpm
Sliding speed	4.7 m/s
Axial load	140 kN - at the surface at 270 rpm, 225 kN - at the depth of 180 m at 270 rpm
Specific load	1.9 MPa/3.1 MPa
Lubricant	Shell Gadinia 40(equivalent to ISO VG-150)

$$h_{min} = \sqrt{FC \times \frac{U \times \eta_{eff} \times L^2 \times B \times Z}{F}} = 15.9 \times 10^{-6}m \tag{3}$$

$$T_b = fc \times \frac{U^2 \times \eta_{eff}}{k \times h_{min}} + T_{amb} = 76.7^\circ C \tag{4}$$

where: FC – coefficient describing the film geometry, which is separately calculated using a procedure described in [17], which is equal to 0.067 in this case

U – sliding speed [m/s]

$\eta_{eff}$  – efficient oil viscosity, calculated according to the standard, equal to  $27 \times 10^{-3}$  Ns/m<sup>2</sup>

L – bearing pad length [m]

B – bearing pad width [m]

Z – number of bearing pads

F – bearing maximum load (225000 N)

k – heat dissipation coefficient, taking into account bearing housing surface and bearing pads surface, calculated according to the standard, equal to 538.3 W/m<sup>2</sup>K

fc –coefficient of bearing losses, calculated according to the standard, equal to 0.791

According to the above calculation, the minimum film thickness (15.9 μm) is considerably greater than the limiting value (10.7 μm), and its temperature is considerably lower than the limiting value equal to 90 °C, so the bearing failure most probably did not occur because of too demanding operational conditions.

As mentioned above, the bearing is of standard design, therefore its operating parameters can be compared to those of stock bearings produced by specialised manufacturers. According to the catalogue [18], a bearing with an equivalent outer diameter is the 17-inch bearing, which, according to the selection chart (Fig. 8) has a load carrying capacity of approximately 180 kN. This value is considerably more than the submarine bearing load at the surface, equal to 140 kN and somewhat less than the submarine bearing load in full submersion. Since the data in the graph is presented assuming a much lower lubricant viscosity - ISO VG-32 supplied at 50 °C, the submarine bearing load can be considered normal for its dimension, rotational speed and oil viscosity. On the other hand, the load should not be considered as low because, contrary to the analysed thrust bearing, the catalogue bearing of this particular manufacturer is equipped with a system of levers equalizing the load distribution among pads.

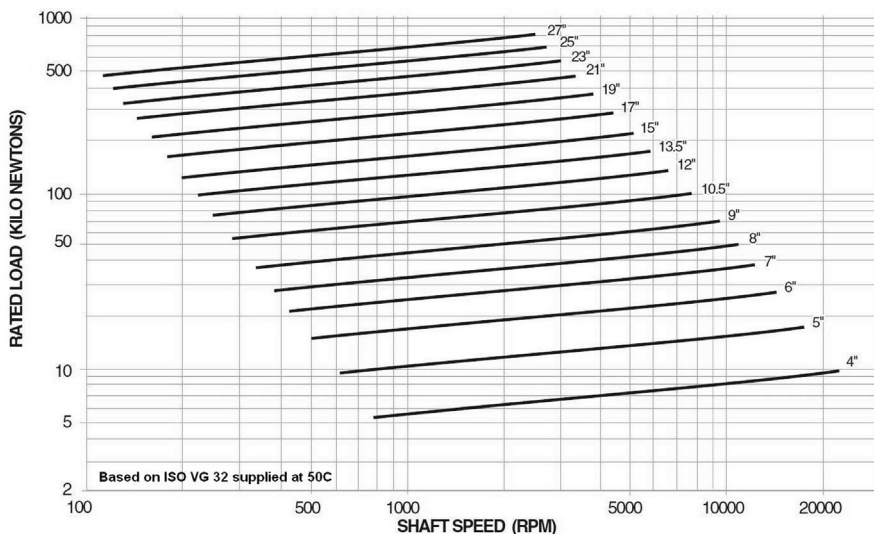


Fig. 8. Bearing selection chart showing load of contemporary industrial tilting pad thrust bearings [18].

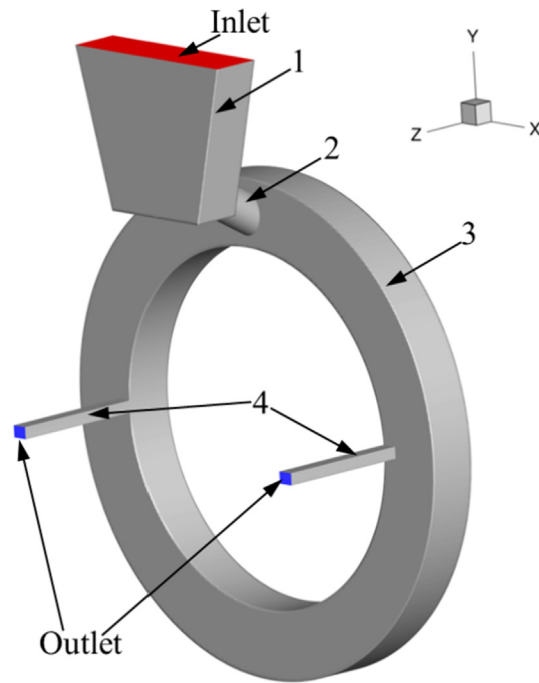


Fig. 9. Simplified geometry of the lubricating system for CFD calculations.

## 6. Lubrication system analysis

Operation of the lubrication system described above, depends on oil viscosity, which in turn depends on temperature and centrifugal force, which further depends on rotational speed. Oil flow is also dependent on the complex geometry of the bearing housing interior. Due to this complexity, the performance of this system can only be precisely determined in experiments, which is difficult. However, with some assumptions, a relatively simple calculation model for the RANS numerical simulation can be built (Fig. 9).

The assumptions can be grouped in four categories:

- A. Geometry simplification - geometry of the channel through which oil flows to the thrust bearing is simplified to the geometry shown in Fig. 9, composed of a trapezoidal pocket (number 1 in Fig. 9), an inclined circular hole (no 2), a ring shaped channel of rectangular cross-section (no 3) and two axial grooves of rectangular cross-section (no 4);
- B. Operational parameters deduced from the principle of operation –
  - The thrust collar delivers an adequate amount of oil to the pocket (no 1), so that the pocket is completely filled with oil – this assumption enables to evaluate maximum possible output of the lubricating system;
  - Oil flows through the lubricating system due to gravity only, thus pressure is generated by the height of the liquid column equal to the radius of the thrust collar and the pocket – 0.2 m;
  - after passing the grooves, oil exits to the space between tilting pads and is further distributed to other pads by the rotating collar, thanks to centrifugal and viscosity forces;
- C. Oil parameters: the viscosity and density of the oil are the same as the viscosity of the ISO VG-150 oil (the exact viscosity vs temperature characteristic of Shell Gadinia 40 oil was unknown);
- D. Assumptions usually taken in flow calculations: the flow through the lubricating system is laminar (Reynolds number in grooves, where velocity is the highest is equal to 5), oil temperature is constant, flow is incompressible.

An unstructured hexahedral grid of 275 000 cells, created in Numeca Hexpress [19] was used for numerical calculations. Steady-state calculations were carried out with Ansys Fluent [20] code using the SIMPLE scheme with 2nd order spatial discretization. In order to reduce the computation cost, model YZ symmetry was assumed and calculations were performed for half of the model.

The streamlines of oil are shown in Fig. 10.

The results obtained using the numerical simulation are shown in Fig. 11, where the velocity fields in particular parts of the system are presented in the form of additional graphs (parabolic distribution indicates laminar flow). In Fig. 12, the maximum speed of oil in particular parts of the system is shown. One can see that the axial grooves are the segments in which the oil velocity is greatest – reaching 0.3 m/s, while in the inclined hole it is lower than 0.1 m/s.

The system output considering a viscosity of 290 mm<sup>2</sup>/s at 30 °C, is equal to 0.85 l/min. Since the flow is directly proportional to oil viscosity, it can be re-calculated for various oil viscosities. The results are shown in Table 2.

On the other hand, the calculation method presented in the ISO Standard No 12,130 [12] allows for the evaluation of the

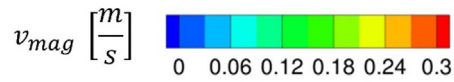
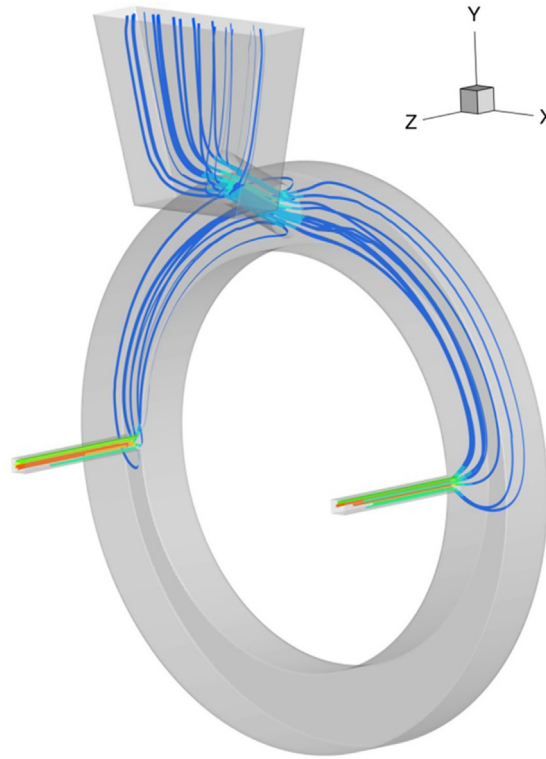


Fig. 10. Oil streamlines in the lubricating system.

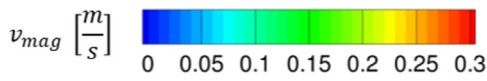
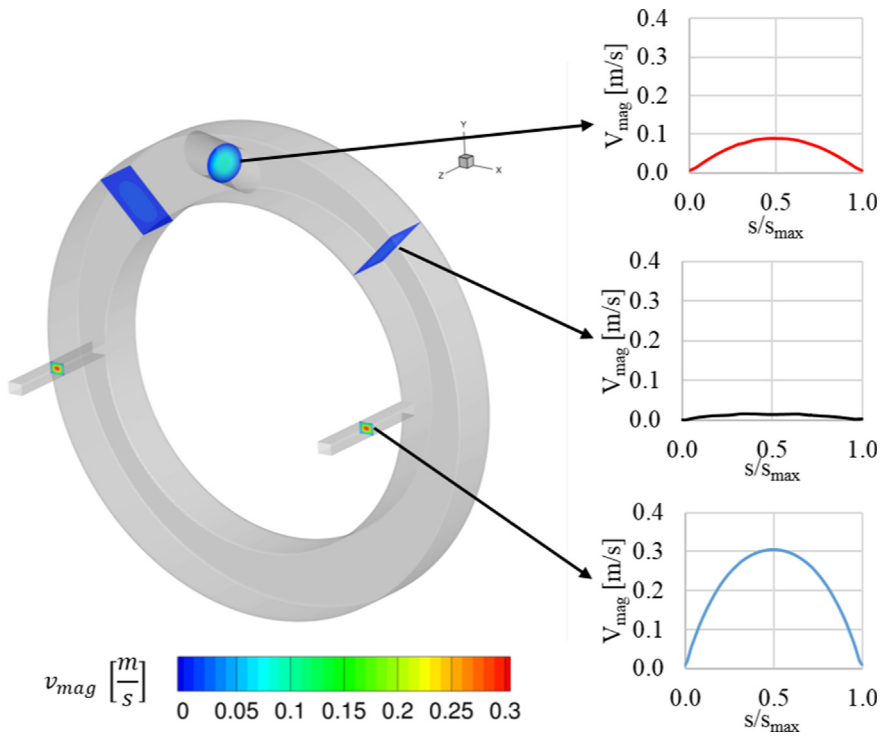


Fig. 11. Oil velocity distribution in particular parts of the lubricating system.



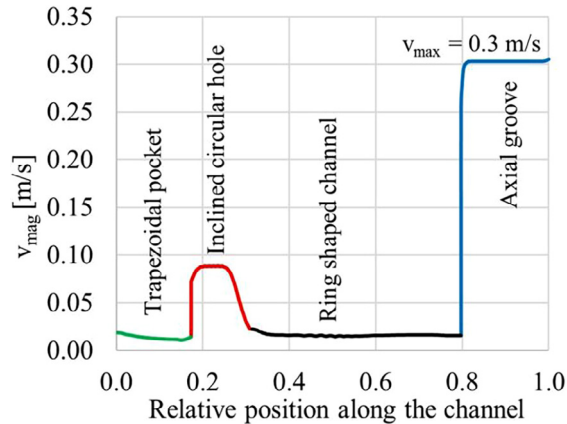


Fig. 12. Maximum oil velocity along the lubricating system.

**Table 2**  
Lubricating system output at different oil viscosity.

Temp [°C]	Viscosity [mm <sup>2</sup> /s]	Supply [l/min]
20	510	0.49
30	290	0.85
40	150	1.65
50	90	2.75
60	60	4.13

necessary flow rate in the thrust bearing, with the use of the following formula (5)

$$Q = Q1 \times B \times h_{min} \times U \times z \quad (5)$$

where  $B$  – bearing pad width, equal to 95 mm

$h_{min}$  – minimum film thickness – 21.5  $\mu\text{m}$  (calculated acc. to [17] for the load of 140 kN)

$U$  – sliding speed, equal to 3.9 m/s for 210 rpm

$Z$  – number of pads, equal to 9

$Q1$  – coefficient for the amount of oil entering the pad equal to 0.568 (calculated acc. to [17]).

The necessary flow rate is almost linearly dependent on the rotational speed. Substituting the minimum film thickness of 16  $\mu\text{m}$  and other data of the analyzed thrust bearing, it is approximately equal to 2.4 l / min. The required flow rate for other speeds is shown in Table 3. Whilst comparing the results of oil supply and demand calculated with the usage of the ISO standard, a major discrepancy can be observed, with theoretical demand being much greater than the oil supply for the lubricating system. The demand, calculated on the optimistic assumption of an oil gap completely filled with oil, seems to be significantly overestimated, since the bearing was operating properly in the commissioning tests run at 30 °C and rotational speed of 210 rpm. Using this information, the oil demand result can be recalculated, assuming the same proportion of demand and supply at other rotational speeds. The results are shown in the third column of Table 3 and in Fig. 13. The result also shows that 30 °C is most probably the accurate temperature for bearing operation at the maximum shaft speed of 270 rpm, with a clear margin of safety, however at 20 °C, rotational speeds above 140 rpm should be avoided.

## 7. Conclusions

After a submarine thrust bearing failure, the design and performance of its autonomous lubricating systems were analysed. The bearing design was found to be both standard and adequate for its purpose. The load did not exceed that of similarly designed

**Table 3**  
Required oil flow through the thrust bearing as a function of rotational speed.

Rotational speed [rpm]	Theoretical demand [l/min] according to ISO 12130	Corrected demand [l/min]
110	1.12	0.40
160	1.78	0.63
210	2.42	0.85
270	3.21	1.13

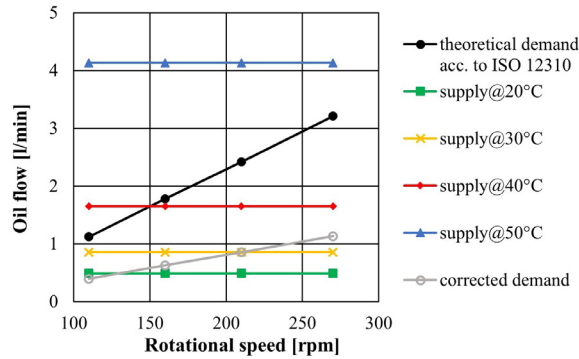


Fig. 13. Comparison of the lubricating system output at various oil temperatures (horizontal lines) with theoretical and corrected bearing requirement.

bearings.

The bearing was lubricated using an autonomous lubricating system in which gravity generates static pressure that causes the oil to flow. The output of the system was evaluated using numerical simulations for a simplified system geometry. The system's flow resistance is dependent on oil viscosity, therefore also on its temperature. The calculations show, that the oil flow was probably too small to meet the bearing demand in conditions of high shaft speed and low oil temperature. These findings can be also supported by the bearing photographs taken after damage was done, where only the pads that are closest to the lubricating system's output show visible blackish traces of burnt oil.

As countermeasures to avoid such failures in future, certain suggestions were made:

1. Use of oil with higher viscosity index, for example a standard motor oil of 10 W/40 or 5 W/30 SAE viscosity class, will meet the requirements
2. Since the bearing is not overloaded, the use of less viscous oil grades, such as ISO VG-68 or ISO VG-100, will allow safe operation at temperatures below 30 °C
3. Installation of an oil heater in the oil sump, which will heat the oil once its temperature falls below a certain level.
4. Since the axial grooves cause major resistance to flow, increasing their cross section should also help in increasing the system output.

## Declaration of Competing Interest

The authors declared that there is no conflict of interest.

## References

- [1] J.E.L. Simmons, N. Henderson, Developments in naval thrust bearings, *J. Naval Eng.* 32 (1990) 344–353.
- [2] Propulsion Motor Bearings and Thrust Bearings for Naval Application (Submarines). From <http://gearconsult.no/wp-content/uploads/2016/08/Propulsion-Motor-Bearings-and-Thrust-BearingsSubmarine.pdf> (access 27.10.2019).
- [3] C. Howard, Technologies for the Management of the Acoustic Signature of a Submarine. Proceedings of the Submarine Institute of Australia 2010 (2010).
- [4] D. Xu, B. Han, W. He, Z. Cheng, Review of advances on longitudinal vibration of submarine propulsion shafting and its vibration reduction technology, *Vibroengineering PROCEDIA* 10 (2016) 52–57.
- [5] P.G. Dylejko, N.J. Kessissoglou, Y. Tso, C.J. Norwood, Optimisation of a resonance changer to minimise the vibration transmission in marine vessels, *J. Sound Vib.* 300 (2007) 101–116.
- [6] G.K. Rightmire, V. Castelli, D.D. Fuller, An experimental investigation of a tilting-pad, compliant-surface, thrust bearing ASME, *J. Lubrication Tech.* 98 (1) (1976) 95–110, <https://doi.org/10.1115/1.3452789>.
- [7] Michell Bearings Webpage <https://www.michellbearings.com/product/thrust-blocks> (29.11.2019).
- [8] M. Fonte, P. Duarte, V. Anes, M. Freitas, L. Reis, On the assessment of fatigue life of marine diesel engine crankshafts, *Eng. Fail. Anal.* 56 (2015) 51–57.
- [9] H. Iliev, Failure analysis of hydro-generator thrust bearing, *Wear* 225 (1999) 913–917.
- [10] L.A. Teran, C.V. Roa, J. Muñoz- Cubillos, R.D. Aponte, J. Valdes, F. Larrahondo, S.A. Rodríguez, J.J. Coronado, Failure analysis of a run-of-the-river hydroelectric power plant, *Eng. Fail. Anal.* (2016) 87–100, <https://doi.org/10.1016/j.engfailanal.2016.05.035>.
- [11] Instruction Manual of Kobben type submarine (SJP1220) – translation to Polish – (1992).
- [12] C.R. Gagg, P.R. Lewis, Wear as a product failure mechanism – Overview and case studies, *Eng. Fail. Anal.* 14 (2007) 1618–1640.
- [13] W.F. Durand, Aerodynamic Theory. (1935) 174, <https://doi.org/10.1007/978-3-642-91487-4>.
- [14] C.F. 'O' Class Submarines, Training Notebook, Introduction and Construction (1956) <http://www.hnsa.org/doc/oberon/propellers/index.htm#pg193> (30.11.2019).
- [15] Shell marine engine oils: <https://www.shell.com/business-customers/marine/marine-lubricants/engine-oils.html> (access 30.11.2019).
- [16] Oil viscosity charts – from [https://www.skf.com/binary/21-120917/0908%25200070%2520-%252010000%2520w\\_tcm\\_12-120917.png](https://www.skf.com/binary/21-120917/0908%25200070%2520-%252010000%2520w_tcm_12-120917.png) (access 7.02.2020).
- [17] International Standardization Organization: Plain Bearings - Hydrodynamic Plain Tilting Pad Thrust Bearings under Steady-State Conditions. Part 1-3. ISO 12130.
- [18] Equalizing Thrust Bearings – comprehensive design catalogue <https://www.kingsbury.com/pdf/catalog-eqh.pdf> (access 29.11.2019).
- [19] HEXPRESSv3.1 Unstructured Grid Generator User Manual (2014).
- [20] Ansys Fluent 2019 User Guide (2019).